Journal of Physical Science, Vol. 17(2), 15–26, 2006 

# MODELLING AND SIMULATION STUDY OF VISIBLE EMISSION TRANSMISSIVITY OF SILICON RELATED TO SINGLE AND MULTILAYER ANTIREFLECTION COATINGS

Kifah Q. Salih and M.R. Hashim*

Solid State and Applied Physics Group, School of Physics,
Universiti Sains Malaysia, 11800 USM Pulau Pinang, Malaysia

*Corresponding author: roslan@usm.my

**Abstract:** *In this study, the effect of single and multilayer thin film coatings at the central wavelength 720 nm on the transmissivity of silicon as active medium has been investigated. A model, based on the Transfer Matrix Method (TMM) of multilayer is used to evaluate the transmittance of Si as active medium (emitter) at 720–750 nm when Ge,* $SiO_2$ *and Si are used as single and multilayer thin film coatings. The results of this simulation study lead to the following conclusions: the transmissivity of ~ 720–750 nm emission of silicon is affected significantly by the single and multilayer thin film coatings of Ge,* $SiO_2$ *and Si/*$SiO_2$*/air and Si/Ge/Si/*$SiO_2$*/air show high transmissivity of 92% and 100% at 720 nm respectively. Uncoated Si (active medium) surface shows low transmissivity of 66%. The width of the high-transmittance region of Si/Ge/Si/*$SiO_2$*/air is less than Si/*$SiO_2$*/air at 720 nm.*

**Keywords:** antireflection coatings, silicon active medium, transmissivity

## 1. INTRODUCTION

Crystalline Silicon (c-Si) is an indirect semiconductor and has little efficiency in light emission. However, the optical properties of porous Si (p-Si) are significantly different from those of bulk c-Si. p-Si is actually a nanocrystalline material. It has dimensions in the low nanometer range. Canham [1] reported that if the structure size reaches a value on the order of < 5 nm, quantum effects can occur and in fact these effects cause the strong visible PL in the region 1.4–2.2 eV. Nanocrystallite Si has been studied extensively because it would open a new possibility for indirect-gap semiconductors as new materials for optoelectronic applications. The transmissivity of Si emission at the air-silicon is low due to the large refractive index discontinuity that exists at the air-silicon range [Fig. 1(a)]. By placing a single layer of antireflective coating (AR) of intermediate refractive index on the silicon surface, this large index discontinuity is broken into two smaller steps [Fig. 1(b)], resulting in a lower broadband reflectivity. Further reduction in broadband reflectivity can be achieved by adding additional intermediate index layers, thus

breaking the air-silicon index discontinuity into smaller and smaller steps. Therefore, a gradient index AR is the limit of this progression, where a single index discontinuity is replaced by a continuous transition from high to low index material (air) as shown in Figure 1(c). If this continuous index transition occurs over several wavelengths of optical path length, broadband reflectivity approaching zero can be achieved [2].

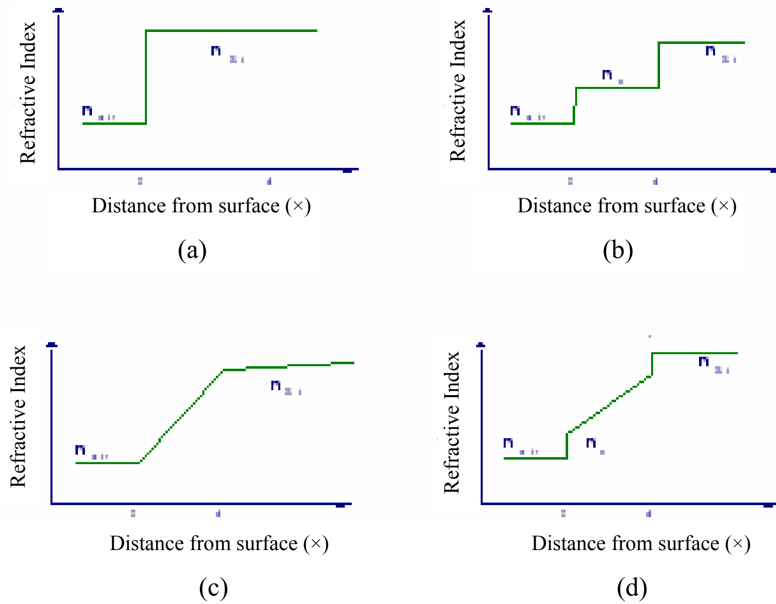


Figure 1: Four basic spatial refractive index profiles of thickness *d*: (a) No AR film, (b) single layer AR film, (c) linear graded AR film, and (d) AR film with a partial gradient ($n_x$ is arbitrary)

Graded refractive index profile i.e., $n = n\ (\lambda, d)$, where $d$ is the depth from the surface, offers the best performance. Different kind of paraboloid or exponential refractive index profiles can give very broad transmission bands. Single-layer antireflections coatings are generally deposited with a thickness of $\lambda/4$, where $\lambda$ is the desired wavelength for peak performance. Since the refractive index of air is 1.0, the thin antireflection film ideally should have a refractive index of $\sqrt{n_{\text{substrate}}}$ [3–5]. There is no ideal material that can be deposited in durable thin layers with a low enough refractive index to satisfy this requirement exactly [3]. These coatings are still more theoretical than practical solution because refractive index gradients are difficult to control during fabrication. In this paper, we explain the model and basic formula of single and multilayer

antireflection coatings of Si, $SiO_2$ and Ge for increasing transmittance of Si as active medium in the far red region of 720–750 nm. This paper reports the design and simulation of the transmissivity of single and multilayer coatings; and also reports the results of each design at the central wavelength 720 nm.

## 2. MODELING AND SIMULATION

The knowledge of thickness and refractive index of AR coatings on semiconductor material surface is a key issue for increasing the performance efficiency of emitters such as output intensity, monochromaticity. Single and multilayer antireflection coatings are designed to increase material surface transmission and reduce surface reflection over a specific wavelength range. The transmittance curves can be calculated with the transfer matrix method for as many AR layers as desired using MATLAB software. In the case of silicon as emitter, the radiation are emitted in all directions. The main loss mechanism of emitter in the material is due to defects, surface roughness and emitter-air interface properties (contacts and the reflectivity). This latter loss is very significant as silicon has relatively high refractive index as shown in Figure 2.

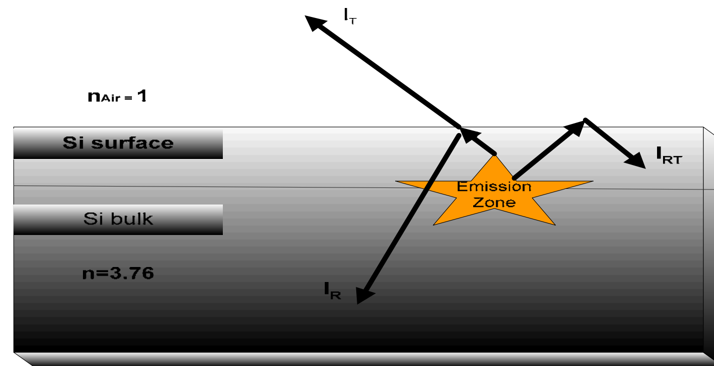


Figure 2: A schematic illustrating the main optical losses mechanism of emission light at Si/air interface

Of the radiation emitted in the forward direction, that striking the front surface at an angle $\theta > \sin^{-1}(1/n)$ will suffer total internal reflection $I_{RT}$. Hence, emitted radiation in a cone of half-angle less than this value will be capable of being emitted, that is $I/2n^2$ of the radiation emitted ($I_E$) in the forward half-sphere. This radiation will suffer partial reflection ($I_R$), given for near normal incidence by Fresnel's law as [6–8]:

$$\frac{I_R}{I_E} = \left(\frac{n-1}{n+1}\right)^2 \tag{1}$$

In our optical model for increasing the transmissivity of visible emission of Si related to Figure 2, the contribution of the single and multilayer antireflection coatings are calculated using the transfer matrix method at the central wavelength 720 nm (where incident angle of emitted light at Si/air interface is $\theta = 0$). In the calculation, we use theoretically determined optical thickness ($d$) of all materials with $n_{Si} = 3.76$, $n_{SiO_2} = 1.455$, $n_{Ge} = 4.897$. Single-layer AR coatings are generally deposited with a thickness of $\lambda 4$, where $\lambda$ is the desired wavelength for peak performance; in our study $\lambda$ is 720 nm.

In the study, we propose Si as a simple rectangular diode geometry in the far red region of 720–750 nm which is so easily fabricated by scribing and cleaving with this wavelength design, so we can explain our modeling using Figure 2 at Si/air interface only or Si surface-AR coatings interface (single or multilayer). A plain wave (emission wave from Si) interacting with a stack of thin layers is considered, so [9,10]:

$$E = E_0\, e^{ikr-i\omega t} \qquad H = H_0\, e^{ikr-i\omega t} \tag{2}$$

Where $E$ and $H$ are the electrical field and the magnetic field strengths, respectively, $E_0$ and $H_0$ are their amplitudes, $k$ is a wave vector and $\omega$ is the frequency of the incident light. We let the thin layers to have different refractive indices.

Inside each layer, the related Maxwell's equations are [9,10]:

$$k \times E_0 = (-\,\omega/c) \times H_o \qquad k \times H_0 = (-\omega n^2/c) \times H_0 \tag{3}$$

The boundary conditions at the interface of two layers having different refractive indexes $n_1$ and $n_2$ are:

$$(E_0)_{\tau 1} = (E_0)_{\tau 1} \qquad n_1(e_k \times E_0)_{\tau 1} = n_2(e_k \times E_0)_{\tau 2} \tag{4}$$

Where the subscript $\tau$ denotes the tangential component with respect to the boundary and $e_k$ shows the direction of the wave propagation. For simplicity, we consider normal incidence of light with plane polarization ($\theta = 0$). So, $N$ layers of $n_j$ can be expressed in terms of the field ($E$) [9–10]:

$$\begin{pmatrix} E+ \\ E- \end{pmatrix}_{final} = (\hat{S}_a)^{-1}\hat{B}_N\hat{B}_{N-1}\hat{B}_{n-2}...\hat{B}_1\hat{S}_a \begin{pmatrix} E+ \\ E- \end{pmatrix}_{initial} \tag{5}$$

Where the subscript $a$ is related to the environmental area, $\hat{S}$ are the surface matrices:

$$\hat{S}_j = \begin{pmatrix} 1 & 1 \\ n_j & -n_j \end{pmatrix} \tag{6}$$

Where, $\hat{B}$ is the layers' matrices:

$$\hat{B}_j = \hat{S}_j\hat{\Phi}_j(\hat{S}_j)^{-1} = \begin{pmatrix} \cos j_j & i\dfrac{\sin j_j}{n_j} \\ in_j\sin j_j & \cos j_j \end{pmatrix} \tag{7}$$

Where $\Phi$ is the diagonal phase matrix connecting the fields $E_j$ ($z$) at the opposite surfaces of the layer $j$, $\varphi_j$ is equal [9,10]:

$$\varphi_j = n_j \frac{\omega}{c} d_j \ \ n_j \tag{8}$$

Where $d_j$ is the layer thickness and $k_j = n_j\omega/c$ is the wave number of the $j$-th layer. Each layer is considered separately. Thus, the transmission can be expressed in term of field $E$ [9]:

$$T = \left|\frac{(E_+)_f}{(E_+)_i}\right|^2 = |t|^2 \tag{9}$$

Equation (9) can be expressed as [10]:

$$Y = \frac{C}{B} \tag{10}$$

Where $Y$ is the optical admittance and $B$ and C are the total magnetic and total electric amplitude of the light propagation in the medium, respectively. So, the transmittance ($T$) can be explained in term of $Y$ as below:

$$T = \frac{4Y_o Re(Y_{sub})}{(Y_o B + C)(Y_o B + C)} \tag{11}$$

## 3. RESULTS AND DISCUSSION

The transmissivity curves in the far red region 720–750 nm of electromagnetic spectrum for antireflection coatings of Si/air, Si/Ge/air, Si/$SiO_2$/air, Si/Ge/$SiO_2$/air, Si/$SiO_2$/Ge/air, Si/Ge/Si/air, Si/Ge/Si/Ge/air, Si/Ge/Si/$SiO_2$/air and Si/$SiO_2$/Si/$SiO_2$/air AR coating structures as single layer and multilayer thin film coatings have been simulated and plotted in Figures 3–12. Please note that the maximum transmittance is obtained from Figure 11 of Si/Ge/Si/$SiO_2$/air.

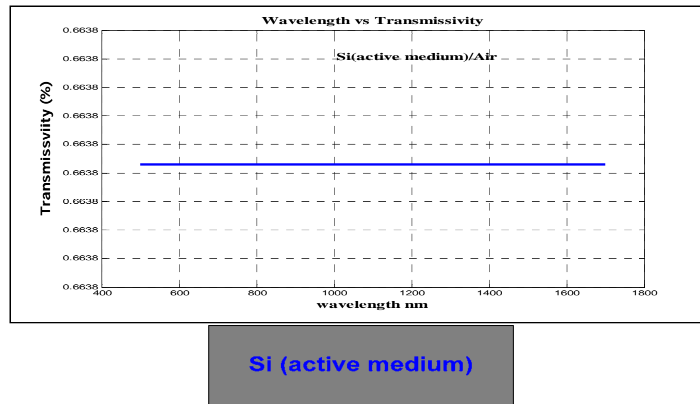


Figure 3: Simulated transmissivity for Si/air at $\lambda$ = 720 nm: $n_{Si}$ = 3.76, $n_{air}$ =1.0 (i.e., uncoated Si surface)

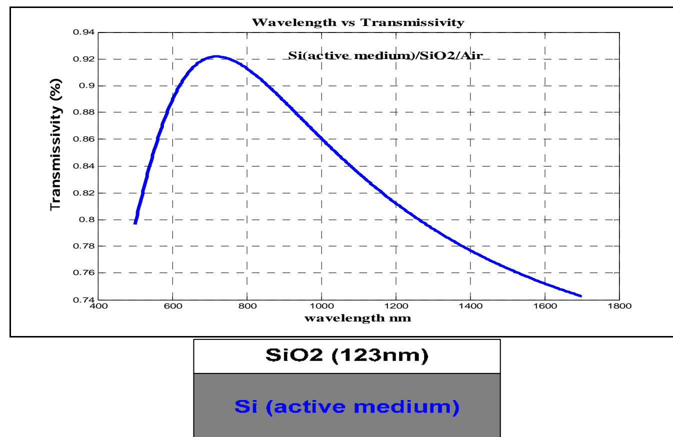


Figure 4: Simulated transmissivity for Si/$SiO_2$/air. $SiO_2$ layer is $\lambda$/4 thick at $\lambda$ = 720 nm: $n_{SiO_2}$ = 1.455

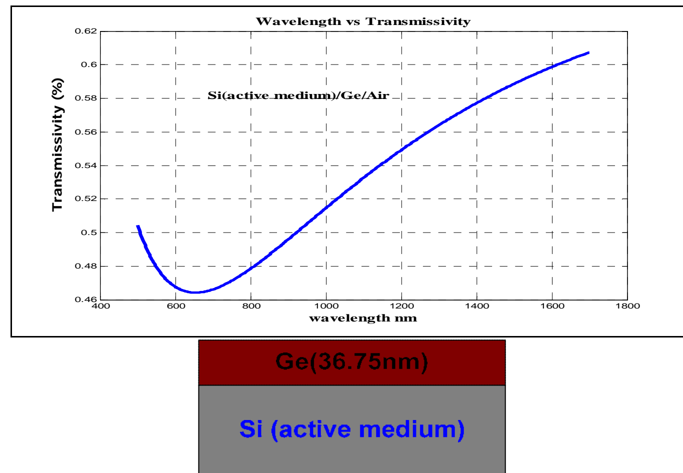


Figure 5: Simulated transmissivity for Si/Ge/air. Ge layer is $\lambda$4 thick at $\lambda = 720$ nm: $n_{\mathrm{Ge}} = n_H = 4.897$

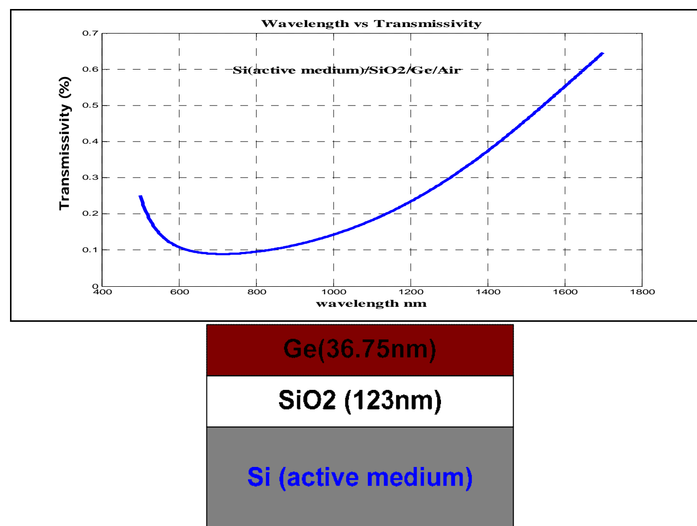


Figure 6: Simulated transmissivity for Si/$SiO_2$/Ge/air. Layers are $\lambda/4$ thick at $\lambda = 720$ nm: $n_{\mathrm{Si}} = 3.76$, $n_{\mathrm{SiO_2}} = 1.455$, $n_{\mathrm{Ge}} = n_H = 4.897$

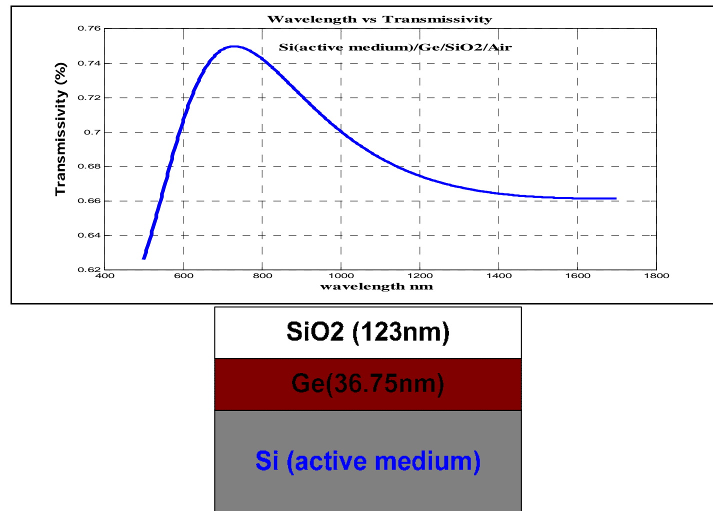


Figure 7: Simulated transmissivity for Si/Ge/$SiO_2$/air. Layers are $\lambda/4$ thick at $\lambda = 720$ nm: $n_{Si} = 3.76$, $n_H = 4.897$, $n_L = 1.455$

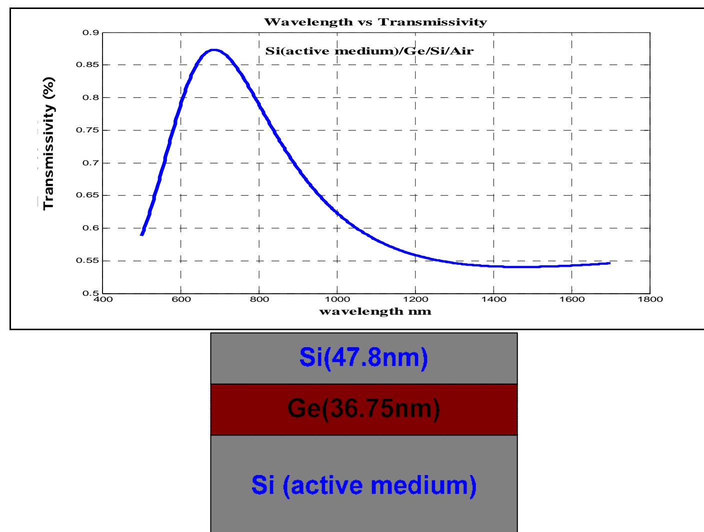


Figure 8: Simulated transmissivity for Si/Ge/Si/air. Layers are $\lambda/4$ thick at $\lambda = 720$ nm: $n_{Si} = 3.76$, $n_H = 4.897$, $n_{Si} = 3.76$

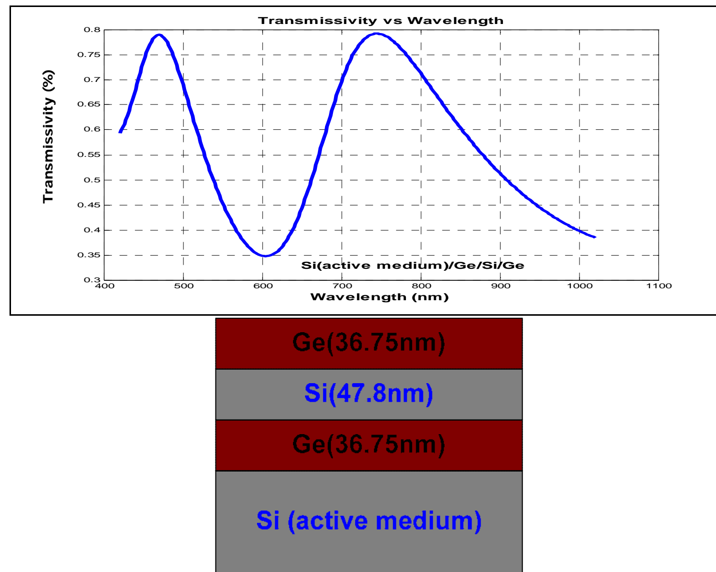


Figure 9: Simulated transmissivity for Si/Ge/Si/Ger/air. Layers are $\lambda/4$ thick at $\lambda = 720$ nm: $n_{\mathrm{Si}} = 3.76$, $n_H = 4.897$, $n_{\mathrm{Si}} = 3.76$

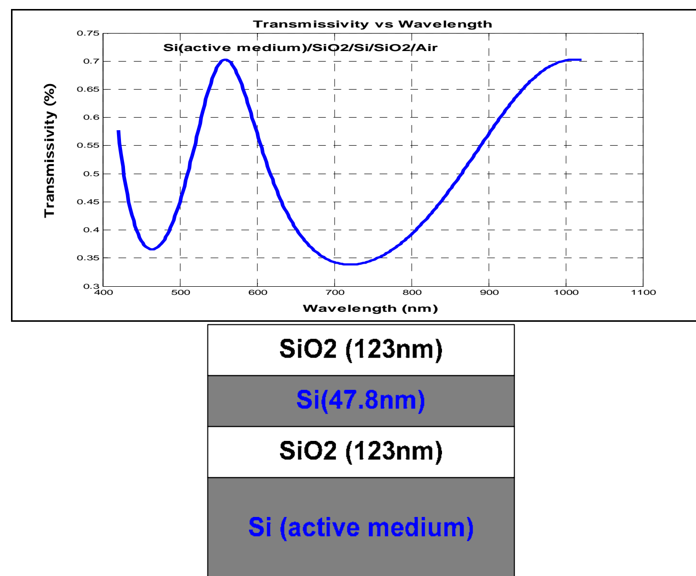


Figure 10: Simulated transmissivity for $Si/SiO_2/Si/SiO_2$/air. Layers are $\lambda/4$ thick at $\lambda = 720$ nm: $n_{\mathrm{Si}} = 3.76$, $n_L = 1.455$

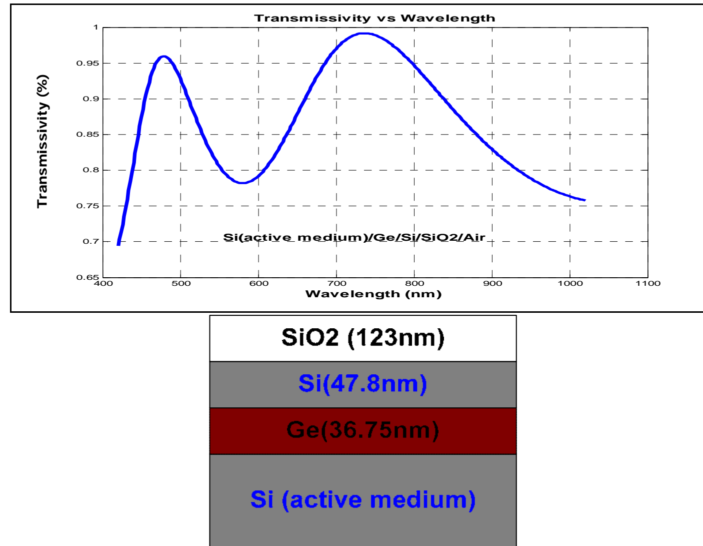


Figure 11: Simulated transmissivity for Si/Ge/Si/$SiO_2$/air. Layers are $\lambda/4$ thick at $\lambda = 720$ nm: $n_H = 4.897$, $n_{Si} = 3.76$

In the curves of Figures 4, 7 and 8, the width of the high-transmissivity region decreases while its height increases, due to the refractive index difference ($\Delta n$) between AR coatings materials. The difference between the curves of Figure 4 and Figure 11 is caused by the refractive index difference at interfaces as illustrated in regions 1(c) and 1(d) and region 2(b) of Figure 12.

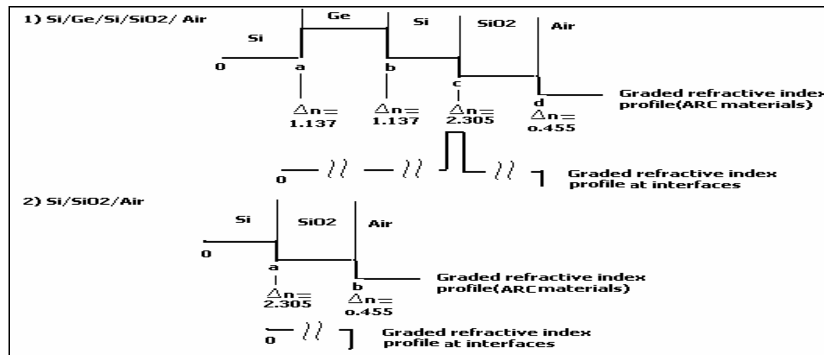


Figure 12: A schematic diagram illustrating the graded refractive index profile of Si/Ge/Si/$SiO_2$/air and Si/$SiO_2$/air antireflection coating structure

These curves show good transmissivity due to the refractive index difference at interfaces, i.e., at $SiO_2$-air interfaces [1(d) and 2(b), Fig. 12] as well as due to the insertion of an extra Si layer between the periodic structures. Figures 9–11 show blue transmissivity at about 440–490 nm. In particular, Figure 11 shows high blue transmissivity (~96%) at 480 nm because the rejection zone ($2\Delta g$) is solely a function of the indices of the two materials used to construct the multilayer in the case of a quarter wave stack with layers of refractive index $n_L$ and $n_H$. So, we can expressed our results from the figures in term of the width of the rejection zone ($2\Delta g$):

$$\Delta g = 2/\pi \sin^{-1} (n_H - n_L) / (n_H + n_L), \tag{12}$$

Figure 11 shows good result in such that: by reduction of rejection zone in the total amount of material will reduce the losses due to residual absorption in the materials and thus increase the transmittance.

## 4. CONCLUSION

In this paper, we presented the simulated transmissivity of Si as emitter using the transfer matrix method. This method directly calculates the theoretical optical transmissivity values of the far red emission of Si using only refractive indices and thickness of coating materials from Si, $SiO_2$ and Ge. The maximum transmissivity of Si in 720–750 nm region of the electromagnetic spectrum can be obtained with insertion of an extra Si layer between the periodic structures of alternately high and low index of Ge and $SiO_2$ as evident from Figure 11.

## 5. REFERENCES


1. Canham, L.T. (1990). *Appl. Phys. Lett.*, 57, 1046–1048.
2. Jacobsson, R. (1997). In E. Wolf (Ed.). *Progress in optics.* Vol. 5. New York: John Wiley & Sons, 249.
3. Coating theory. Single-Layer Antireflection Coatings. www.mellesgriot .com/products/optics/oc_2_2.htm (accessed January 10, 2005).
4. Southwell, W.H. (1983). *Optics Letters*, 8, 584.
5. Berning, P.H. (1962). *J. Opt. Soc. Am.*, 52, 231.
6. Heavens, O. (1970). *Thin film physics.* London: Methuen.
7. Glang, R. & Maissel, L.I. (1970). *Handbook of thin film technology.* London: McGraw-Hill.
8. Jenkins, F.A. & White, H.E. (1976). *The fundamentals of optics.* London: McGraw-Hill.

9. Aroutiounian, V.M., Martirosyan, K.H. & Soukiassian, P. (2004). *J. Phys. D. Appl. Ohys.*, 37(19), L25–L28.
10. Aroutiounian, V.M., Maroutyan, K.R., Zatikyan, A.L. & Touryan, K.J. (2002). *Thin Solid Films*, 517, 403–404.